

Wolfgang Doneit, Ralf Mikut, David Liebetanz, Rüdiger Rupp and Markus Reischl*

Control scheme selection in human-machine-interfaces by analysis of activity signals

DOI 10.1515/cdbme-2016-0153

Abstract: Human-Machine Interfaces in rehabilitation engineering often use activity signals. Examples are electrical wheelchairs or prostheses controlled by means of muscle contractions. Activity signals are user-dependent and often reflect neurological weaknesses. Thus, not all users are able to operate the same control scheme in a robust manner. To avoid under- and overstraining, the interface ideally uses a control scheme which reflects the user's control ability best. Therefore, we explored typical phenomena of activation signals. We derive criteria to quantify the user's performance and abilities and present a routine which automatically selects and adapts one of three control schemes being best suited.

Keywords: calibration; data quality; human-machine interfaces; rehabilitation engineering.

1 Introduction

Human-machine interfaces (HMI) for controlling technical devices in rehabilitation engineering often use electroencephalography (EEG) [1] or electromyography (EMG) [2] to obtain bioelectric signals. Normalization procedures [3] and pattern recognition techniques [4] are used to estimate control signals for devices like electrical wheelchairs [5] or prostheses [6].

A common feature generated from biosignals is the normalized activity signal (e.g. amplitude of a low-pass-filter). Activity signals can also be derived from joystick

axes [7], air pressure with sipping and puffing and positions of shoulders, tongue [8] or head [9].

To generate control signals, commercial systems use robust threshold approaches [10], whereas experimental systems use pattern recognition techniques [11]. A calibration is necessary to adapt the system to the user. Commercial HMIs are adapted mostly by hand.

Ref. [12] presents a wheelchair control interface based on the bilateral recording of myoelectric signals from left and right ear muscle. The raw signals are rectified, filtered and normalized to receive activity signals that correlate with the strength of contractions. The ability to contract the ear muscles is trainable and left and right ear muscle can be activated independently. However, not only training progress is user-dependent, but also extrema and coactivations of the activation signals, dispersion of the intended constant activations, difference between measured and intended activation.

As the control abilities of users vary, users might not only need adapted parameters but also individual control schemes. However, there is only little knowledge about user-specific selections of the control scheme.

Therefore, we propose a method to select a control scheme based on activity signals from a calibration routine. We derive a rule set to assign each user one out of three control schemes. Using benchmark examples we test the method and discuss effects. We provide a real-world dataset to prove functionality.

2 Material and methods

2.1 Calibration routine

If a user is not able to activate two signal channels independently, coactivations occur and control schemes based on difference signals fail. Polynomial regressions approximate the nonlinear relationship of intended activation and measured coactivated signals. Therefore, bilateral calibration routines were proposed in [13, 14] to gather data for model building: The user is asked to simultaneously hold activation levels in two signal channels. The activation levels are the intended activations (intentions)

*Corresponding author: Markus Reischl, Institute for Applied Computer Science, Karlsruhe Institute of Technology, Eggenstein-Leopoldshafen, E-mail: markus.reischl@kit.edu

Wolfgang Doneit and Ralf Mikut: Institute for Applied Computer Science, Karlsruhe Institute of Technology, Eggenstein-Leopoldshafen

David Liebetanz: Department of Clinical Neurophysiology, Georg-August-University, Goettingen

Rüdiger Rupp: Orthopedic Hospital of Heidelberg University, Heidelberg

© 2016 Markus Reischl et al., licensee De Gruyter.

This work is licensed under the Creative Commons Attribution-NonCommercial-NoDerivs 4.0 License.

Bereitgestellt von | KIT-Bibliothek | Karlsruher Institut für Technologie
Angemeldet

Heruntergeladen am | 17.10.16 15:13

$\mathbf{y} = (y_1, y_2)$. The calibration routine records the activation of each channel according to Table 1 for

- single maximal activations of each channel,
- simultaneous maximal activation of both channels,
- single activations of each channel at 50% activation level and
- simultaneous activations of both channels at 50% activation level.

Each of the six calibration steps is described by the membership to a class $z = \{B_1, \dots, B_6\}$ and a vector of intentions $\mathbf{y} = (y_1, y_2)$. The user-generated normalized activation signals are x_1 and x_2 . Table 1 shows the calibration steps, the class membership and intended activations.

2.2 Selection of a control scheme

A control scheme estimates intentions by thresholds or pattern recognition algorithms. We consider three different control schemes:

A *threshold*-based control using one signal channel to recognize intentions given by short/long activations. Sequences comparable to the Morse code are assigned to actions of the rehabilitation device (e.g. turning left or right with a wheelchair). The advantage of the control scheme is its simplicity. Even with coactivations and low abilities of holding an activation level this control scheme is applicable. Disadvantages are time lags in control.

If the user is able to generate better discriminable activation patterns a *classifier*-based control can be applied. A classifier $\hat{z} = f(x_1, x_2; \boldsymbol{\theta})$ is trained for the 6 classes B_i within a calibration B_1, \dots, B_6 and classifies the signals at each time sample. Classes represent intentions, the control scheme maps each intention to an action. No activation in both channels corresponds to a neutral state. Inputs of the classifier are the normalized activation signals x_1 and x_2 . The parameter vector $\boldsymbol{\theta}$ is estimated based on calibration data.

If the user is able to hold different activation levels with both signal channels, a *proportional* control can be

applied. It determines two independent, time-continuous control signals by the level of simultaneous activation of both channels and the difference of both channels (e.g. translational velocity and rotational velocity of a wheelchair). To reduce the influence of unintended coactivations, regression models $\hat{y}_i = f_i(x_1, x_2; \boldsymbol{\theta}_i)$ are used to estimate the continuously valued intention of each channel [13] with the constraints $f_1(0, 0, \boldsymbol{\theta}_1) = f_2(0, 0, \boldsymbol{\theta}_2) = 0$. f_1 and f_2 are polynomial functions of second degree and the parameter vectors $\boldsymbol{\theta}_1$ and $\boldsymbol{\theta}_2$ are estimated by a least squares algorithm. Fluctuating activity signals lead to incessantly changing velocities in the proportional control.

To select an appropriate control scheme three criteria are defined which are also useful for a medical supervisor:

Q_1 describes the ability of the user to generate discriminable activation signals for the classifier-based control scheme. Therefore, we calculate the minimal accuracy of a class for the used classification algorithm

$$Q_1 = \min_j \left(\left(\frac{1}{N_j} \cdot N(\hat{z} = B_j \cap z = B_j) \right) \right). \quad (1)$$

Q_2 quantifies whether the generated signals match the intended activations and describes the ability of the user to generate predetermined activation signals. For a robust estimation of the mean value, the median operator is used. $\tilde{x}_{j,i}$ is the median of the x_i values of all datapoints with class label B_j . $y_{j,i}$ is the intended activation for channel i of all datapoints with class label B_j :

$$Q_2 = \exp \left(-4 \left(\max_{j,i} (\tilde{x}_{j,i} - y_{j,i}) \right) \right) \quad (2)$$

The factor -4 is selected empirically to achieve a smooth course of the criterion. Q_3 quantifies the dispersion of the generated signals. It describes the ability of the user to hold an activation level. For a robust estimation of the dispersion the interquartile range is used. $\tilde{x}_{0.75,j,i}$ is the upper quartile und $\tilde{x}_{0.25,j,i}$ the lower quartile of the x_i values of all datapoints with class label B_j :

$$Q_3 = \exp \left(-4 \left(\max_{j,i} (\tilde{x}_{0.75,j,i} - \tilde{x}_{0.25,j,i}) \right) \right) \quad (3)$$

(4) shows the rules for the selection of an appropriate control scheme.

$$\begin{aligned} (Q_1 > \tau_1) \wedge (Q_2 > \tau_2) \wedge (Q_3 > \tau_3) &\rightarrow \textit{proportional} \\ (Q_1 > \tau_1) \wedge \neg((Q_2 > \tau_2) \wedge (Q_3 > \tau_3)) &\rightarrow \textit{classifier} \\ \neg(Q_1 > \tau_1) &\rightarrow \textit{threshold} \end{aligned} \quad (4)$$

The thresholds τ_1 , τ_2 and τ_3 are selected empirically.

Table 1: Intended activations and classes of the calibration steps.

Calibration step	y_1	y_2	z
1: single x_1	1	0	B_1
2: single x_1 (50%)	0.5	0	B_2
3: single x_2	0	1	B_3
4: single x_2 (50%)	0	0.5	B_4
5: simultaneous x_1 and x_2	1	1	B_5
6: simultaneous x_1 and x_2 (50%)	0.5	0.5	B_6

2.3 Datasets

We simulated three benchmark datasets which represent three states of user performance: Figure 1(A) shows the calibration data of a user with low performance. The data of the calibration steps is overlapping and the dispersion of single classes is high. Figure 1(B) shows the calibration data of a user with medium performance. The dispersion of the classes is high but the classes are discriminable. Figure 1(C) shows the calibration data of a user with high performance. The datapoints of the calibration steps are building small clusters near to their intended activations.

In [14] real-world datasets in a bilateral calibration routine were recorded with antagonistic forearm muscles. Three datasets are generated by one user with varying sensor placements for 12 intentions. Figure 1(D–F) show subsets of the datasets. The subsets correspond to the intended activations of Table 1. The data is preprocessed, i.e. outliers of the calibration steps were already deleted.

3 Results

Analyses were performed with MATLAB and Gait-CAD [15]. Table 2 shows Q_1 , Q_2 , Q_3 and the control scheme selection for the simulated and the real-world datasets

with $\tau_1 = 0.9$, $\tau_2 = 0.15$ and $\tau_3 = 0.5$. The thresholds are empirically selected.

The assessment by the criteria conforms to the description of the benchmark datasets. For dataset 1, Q_1 and Q_3 are below their respective thresholds. Thus, the calibration steps are not discriminable and the dispersion of at least one calibration step is high. The threshold-based control scheme is selected. This evaluation coincides with the visual inspection of dataset 1. With the threshold-based control scheme, the user is at least able to apply several movements even if it takes time. In a classifier-based or a proportional control scheme, the estimated intentions are fluctuating due to the high dispersion in classes and the overlap of different classes. Also for dataset 2, Q_3 is below its threshold. Since the calibration steps are discriminable, the classifier-based control scheme is selected. In this control scheme, the user is able to hold a movement. In the proportional control scheme the velocities are fluctuating due to the high dispersion in classes. For dataset 3, all criteria are above their thresholds. The proportional control scheme is selected.

The real-world datasets look similar to dataset 3 which is appropriate for the proportional control scheme. But the proximity of calibration steps (e.g. B_4 and B_6 in dataset 4 or B_1 and B_5 in dataset 5) leads to a rapid change of velocities by small fluctuations of activation signals in

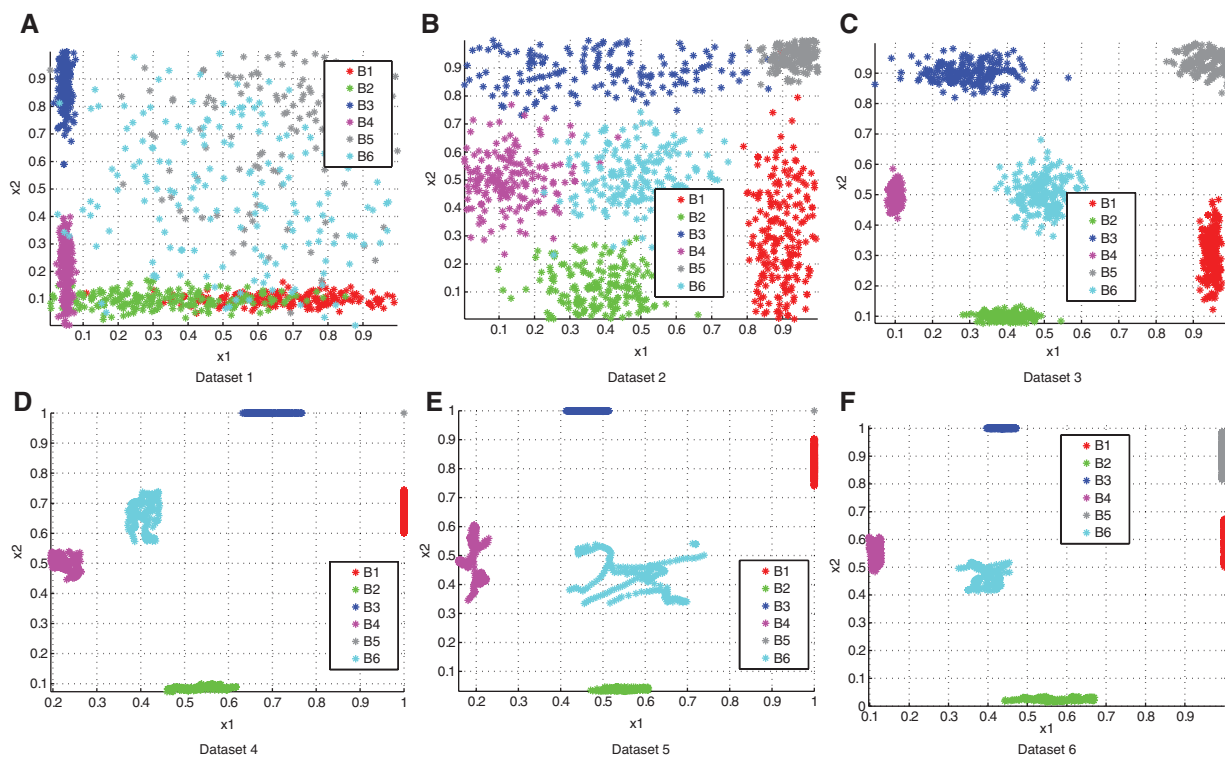


Figure 1: (A)-(C): Simulated datasets representing different levels of user performance. (D)-(F): Parts of the real-world datasets from [14]. Only the calibration steps are used which would have been recorded from the proposed calibration routine.

Table 2: Results for simulated (1–3) and real-world (4–6) benchmark datasets. Values below τ -thresholds are bold.

Dataset	Q_1	Q_2	Q_3	Selection
1	0.556	0.6672	0.2222	<i>threshold</i>
2	0.956	0.2207	0.3065	<i>classifier</i>
3	1	0.3005	0.6583	<i>proportional</i>
4	1	0.064	0.7579	<i>classifier</i>
5	1	0.0372	0.5945	<i>classifier</i>
6	1	0.1742	0.6995	<i>proportional</i>

a proportional control scheme. The calibration steps of the real-world datasets 4, 5 and 6 are discriminable, their dispersions are low and so Q_1 and Q_3 are above their thresholds. For datasets 4 and 5, Q_2 is below its thresholds. That means the data of the calibration steps is different to the intended signals and the proportional control scheme is not appropriate for the user. Instead the classifier-based control scheme is selected. Only for dataset 6 the proportional control scheme is selected.

4 Discussion and outlook

The automatic control scheme selection helps to find a control scheme that fits to the user's performance. Thus, frustration of the user by under- or overstraining can be avoided. The interpretability of the proposed criteria as user performance allows the use in studies and medical investigations. The user performance over several calibrations can be followed and changes in neurological and physiological weaknesses can be quantified. Without our criteria, the information about user performance is lost by using the data just for training a model to estimate intended activations.

The proposed criteria are able to represent different phenomena of activation signal calibration data. The usage of the criteria for selecting an appropriate control scheme has been demonstrated with the help of three simulated and three real-world datasets. The method is currently used to prepare a study regarding user performance evaluation.

Author's Statement

Research funding: The project is funded by the Helmholtz Association (Program bioInterfaces in technology and medicine (RM, MR) and the German Federal Ministry of Education and Research BMBF [WD, DL, RR,MR, Grant No 13EZ1122(A–C)]. Conflict of interest: Authors state no conflict of interest. Informed consent has been

obtained from all individuals included in this study. Ethical approval: The research related to human use complies with all the relevant national regulations, institutional policies and in accordance the tenets of the Helsinki Declaration, and has been approved by the authors' institutional review board.

References

- [1] Millán J, Renkens F, Mourino J, Gerstner W. [Noninvasive brain-actuated control of a mobile robot by human EEG](#). *IEEE Trans Biomed Eng.* 2004;51:1026–33.
- [2] Vitiello N, Olcese U, Oddo CM, Carpaneto J, Micera S, Carrozza MC, et al. A simple highly efficient non invasive EMG-based HMI. *Conf Proc IEEE Eng Med Biol Soc.* 2006;1:3403.
- [3] Knutson L, Soderberg G, Ballantyne BT, Clarke WR. A study of various normalization procedures for within day electromyographic data. *J Electromyogr Kinesiol.* 1994;4:47–59.
- [4] Ciaccio E, Dunn S, Akay M. Biosignal pattern recognition and interpretation systems. *IEEE Trans Biomed Eng.* 1993;12:89–95.
- [5] Choi K, Sato M, Koike Y. A new, human-centered wheelchair system controlled by the EMG signal. *Proc IEEE Int Conference on Neural Networks.* 2006;4664–71.
- [6] Reischl M, Gröll L, Mikut R. [Evaluation of data mining approaches for the control of multifunctional arm prostheses](#). *Integr Comput-Aid E.* 2011;18:235–49.
- [7] Loveless J, Seamone W. Chin controller system for powered wheelchair; 1981.
- [8] Lund M, Christensen H, Caltenco H, Lontis ER, Bentsen B, Andreasen Struijk LN. Inductive Tongue Control of Powered Wheelchairs. *Conf Proc IEEE Eng Med Biol Soc.* 2010;2010:3361–4.
- [9] Min J, Lee K, Lim S, Kwon D. Human-friendly interfaces of wheelchair robotic system for handicapped persons. *Proc IEEE Conf on Intelligent Robots and Systems.* 2002;2:1505–10.
- [10] Otto Bock Orthopädische Industrie. *Patienteninformation für SensorHand.* 646D83; 1999.
- [11] Gopura R, Bandara D, Gunasekara J, Jayawardane T. Recent trends in EMG-based control methods for assistive robots. In: H. Turker, editor, *Electrodiagnosis in New Frontiers of Clinical Research InTech*; 2013. p. 237–68.
- [12] Schmalfuß L, Rupp R, Tuga M, Kogut A1, Hewitt M, Meincke J, et al. Steer by ear: myoelectric auricular control of powered wheelchairs for individuals with spinal cord injury. *Restor Neurol Neurosci.* 2015;34:79–95.
- [13] Doneit W, Tuga MR, Mikut R, et al. [Kalibrierungs- und Trainingsstrategien zur individuellen Signalgenerierung für die myoelektrische Steuerung technischer Hilfsmittel](#). *Technisches Messen.* 2015;82:411–21.
- [14] Stüb L. Entwicklung einer adaptiven Kalibrierungsroutine für zweikanalige EMG-messungen. Bachelorarbeit, Karlsruher Institut für Technologie; 2016.
- [15] Mikut R, Burmeister O, Braun S, Reischl M. The open source Matlab toolbox Gait-CAD and its application to bioelectric signal processing. *Proc DGBMT-Workshop Biosignalverarbeitung.* 2008;109–11.